

 Open access • Journal Article • DOI:10.1103/PHYSREVLETT.61.1591

## Dynamic permeability in porous media. — [Source link](#)

[Ping Sheng](#), [Min-Yau Zhou](#)

**Institutions:** [ExxonMobil](#)

**Published on:** 03 Oct 1988 - [Physical Review Letters](#) (American Physical Society)

Related papers:

- [Theory of dynamic permeability and tortuosity in fluid-saturated porous media](#)
- [Experimental Study of Dynamic Permeability in Porous Media](#)
- [First-principles calculations of dynamic permeability in porous media.](#)
- [Theory of Propagation of Elastic Waves in a Fluid-Saturated Porous Solid. I. Low-Frequency Range](#)
- [New pore-size parameter characterizing transport in porous media.](#)

Share this paper:    

View more about this paper here: <https://typeset.io/papers/dynamic-permeability-in-porous-media-tiu685smdr>

## Dynamic Permeability in Porous Media

Ping Sheng and Min-Yau Zhou<sup>(a)</sup>

*Exxon Research and Engineering Company, Route 22 East, Annandale, New Jersey 08801*

(Received 6 June 1988)

We calculate from first principles the frequency-dependent permeability  $\kappa(\omega)$  in porous media for a variety of microstructures. It is found that when  $\kappa(\omega)$  is scaled by its static value  $\kappa_0$  and the frequency by a characteristic  $\omega_c$  particular to the sample, the resulting function exhibits excellent universal behavior independent of microstructure. We advance arguments that delineate the physical reason for the scaling behavior as well as the condition for its validity. Our predictions are supported by observed correlations in sedimentary rocks and experimental  $\kappa(\omega)$  measurements.

PACS numbers: 47.55.Mh, 47.15.Gf, 47.15.Hg

As one of the basic properties of porous media, permeability has long been recognized for its crucial role in many areas of petroleum and chemical industries ranging from oil production from sedimentary rocks to chemical reactions in zeolites. In recent years, experimental and theoretical studies have uncovered important correlations between permeability and geometric parameters characterizing the microstructure of a porous medium.<sup>1-3</sup> In particular, it was observed that the product of state permeability  $\kappa_0$  and the dc electrical formation factor is directly proportional to a "throat area" measurable by a mercury intrusion experiment,<sup>3</sup> and that in the high-frequency limit the permeability is predicted to contain information regarding the volume-to-surface ratio of a porous medium.<sup>2,4</sup> In light of these findings, it is natural to wonder about the total geometric content of the dynamic permeability function  $\kappa(\omega)$ , defined as  $\mathbf{U}(\omega) = -[\kappa(\omega)/\eta]\nabla p(\omega)$ , where  $\mathbf{U}$  is the average flow velocity,  $\eta$  is the fluid viscosity, and  $p$  is the applied pressure. The answer would determine not only the degree to which permeability can be a good microstructure probe, but also the control one might have on  $\kappa(\omega)$  through microstructure design. In this work, we present results of first-principles calculations of  $\kappa(\omega)$  for a variety of porous microstructures that indicate the general validity of the relation  $\kappa(\omega)/\kappa_0 \approx f(\omega/\omega_c)$ , where  $\omega_c$  is a characteristic frequency of the medium and  $f$  is a universal function independent of microstructure. Physical arguments are advanced to clarify the geometric meaning of this scaling behavior as well as to delineate the general conditions for its validity. Our theory offers a simple explanation for the observed correlations in sedimentary rocks,<sup>3</sup> and the scaling predictions are supported by experimental measurements of  $\kappa(\omega)$ , to be described separately.<sup>5</sup>

Consider a fluid-filled porous medium with bicontinuous solid and fluid networks under the excitation of an external harmonic source with frequency  $\omega$ . The microstructure of a porous medium is generally characterized by a length scale  $a$  that is typical of the pore size. If the fluid has viscosity  $\eta$ , bulk modulus  $K$ , and density  $\rho_f$ ,

then one may also identify an intrinsic time scale  $t_0 = \rho_f a^2 / \eta$ , associated with the viscous relaxation of any fluid excitation, as well as a speed of sound  $c_0 = (K/\rho_f)^{1/2}$ . Since in units of  $a/t_0$  the speed  $c_0$  is almost always a big number (for water in sedimentary rocks with  $a \approx 1 \mu\text{m}$  it is on the order of  $10^3$ ), we have thus identified a dimensionless small parameter  $\epsilon = a/t_0 c_0$  in the problem. By regarding  $L = t_0 c_0$  as a macroscopic length of the system,  $\epsilon$  may alternatively be regarded as the ratio between two length scales. In units of  $a$  and  $\rho_f a^2 / \eta$ , the equations governing the fluid and solid motions under linearized hydrodynamics can be written in the following dimensionless form<sup>6</sup>:

$$-i\bar{\omega}\mathbf{v} = \epsilon^{-1}\nabla \cdot \boldsymbol{\sigma} \quad \text{in } D_f, \quad (1a)$$

$$\boldsymbol{\sigma} = -p\mathbf{I} + \epsilon 2D\nabla\mathbf{v} \quad \text{in } D_f, \quad (1b)$$

$$i\bar{\omega}p = \epsilon^{-1}\nabla \cdot \mathbf{v} \quad \text{in } D_f, \quad (1c)$$

$$-\rho\bar{\omega}^2\mathbf{u} = \epsilon^{-1}\nabla \cdot \boldsymbol{\tau} \quad \text{in } D_s, \quad (1d)$$

$$\boldsymbol{\tau} = \mathbf{C}\epsilon^{-1}\nabla\mathbf{u} \quad \text{in } D_s, \quad (1e)$$

together with the boundary conditions  $\mathbf{v} = -i\omega\mathbf{u}$ ,  $\mathbf{n} \cdot \boldsymbol{\sigma} = \mathbf{n} \cdot \boldsymbol{\tau}$  at the fluid-solid interface. Here  $\bar{\omega} = \omega\rho_f a^2 / \eta$ ,  $\mathbf{v}$  denotes the fluid velocity,  $\mathbf{u}$  the solid displacement,  $\boldsymbol{\sigma}$  the fluid stress tensor,  $\boldsymbol{\tau}$  the solid stress tensor,  $p$  the fluid pressure,  $\mathbf{C}$  the fourth-rank elastic tensor for the solid measured in units of  $K$ ,  $\rho = \rho_s / \rho_f$  the reduced solid density,  $D_f$  the fluid region,  $D_s$  the solid region,  $D\nabla\mathbf{v}$  the symmetrized, traceless, deviatoric part of the  $\partial_i v_j$  matrix, and  $\mathbf{n}$  the unit vector normal to the fluid-solid interface. We have also made the important assumption that the macroscopic pressure gradient ( $p/L$ ) should be on the same order as  $\eta v/a^2$  in accordance with Darcy's law. The unit for the stress field quantities  $p$ ,  $\boldsymbol{\sigma}$ , and  $\boldsymbol{\tau}$  is therefore set to be  $L\eta^2/\rho_f a^3$ . This assumption will be justified by our consistent derivation of Darcy's law from Eq. (1).

Given Eq. (1) with the small parameter  $\epsilon$ , we may apply the well-known technique<sup>6</sup> of homogenization that would enable us to systematically justify the neglect of

the fluid compressibility effect and to decouple the solid displacement from that of the fluid in the permeability calculation. The technique involves the following: (1) the explicit recognition of the two length scales in the problem by writing all the field quantities as a function of  $\epsilon$  plus the two spatial variables  $\mathbf{x}=\mathbf{r}/L$  and  $\mathbf{y}=\mathbf{r}/a$ , and then expanding them as a perturbation series in  $\epsilon$ , e.g.,  $\mathbf{v}=\mathbf{v}_\epsilon(\mathbf{x},\mathbf{y})=\mathbf{v}_0(\mathbf{x},\mathbf{y})+\epsilon\mathbf{v}_1(\mathbf{x},\mathbf{y})+\dots$ ; and (2) letting the gradient operation  $\nabla$  act on both the  $\mathbf{x}$  and the  $\mathbf{y}$  scales, i.e.,  $\nabla=\epsilon\nabla_x+\nabla_y$ , where  $\nabla_{x(y)}$  denotes derivative operation with respect to the  $x$  ( $y$ ) variable. By equating terms with equal powers of  $\epsilon$ , we obtain to the leading order ( $\epsilon^{-1}$ ) the following results. First,  $\nabla_y\cdot\sigma_0=0$ ,  $\nabla_y\mathbf{u}_0=0$ , and  $\sigma_0=-\rho_0\mathbf{I}$ , where  $\mathbf{I}$  is the identity matrix. That means that  $\mathbf{u}_0=\mathbf{u}_0(\mathbf{x})$ , and  $\sigma_0=\sigma_0(\mathbf{x})=-\rho_0(\mathbf{x})\mathbf{I}$  are functions of  $\mathbf{x}$  only. Second,  $\nabla_y\cdot\mathbf{v}_0=0$ ; i.e., *the fluid may be regarded as incompressible on the  $\mathbf{y}$  scale*. This is understandable physically since for  $\bar{\omega}\ll\epsilon^{-1}$ , the acoustic wavelength  $\lambda$  is  $\gg a$ , which implies a negligible compressibility effect on the pore scale. Following Biot,<sup>7</sup> and Burridge and Keller,<sup>6</sup> we define a fluid displacement relative to the solid as  $\mathbf{w}(\mathbf{x},\mathbf{y})=i(\mathbf{v}_0/\bar{\omega})-\mathbf{u}_0(\mathbf{x})$ . Since  $\nabla_y\cdot\mathbf{v}=0$  and  $\mathbf{u}_0(\mathbf{x})$  is independent of  $\mathbf{y}$ , we get  $\nabla_y\cdot\mathbf{w}=0$ . In terms of  $\mathbf{w}$ , the relevant next-order equation<sup>8</sup> (to  $\epsilon^0$ ) is

$$-\nabla_y p_1 - i\bar{\omega}\nabla_y^2\mathbf{w} + \bar{\omega}^2\mathbf{w} = -\nabla_x p_0 - \bar{\omega}^2\mathbf{u}_0. \quad (2)$$

Because  $p_1$  and  $\mathbf{w}$  are solutions to a set of linear equations with the source term  $\nabla_x p_0 + \bar{\omega}^2\mathbf{u}_0$ , they may be formally expressed as  $p_1=\mathbf{P}(\mathbf{x},\mathbf{y})(\nabla_x p_0 + \bar{\omega}^2\mathbf{u}_0)$  and  $\mathbf{w}=\mathbf{W}(\mathbf{x},\mathbf{y})(\nabla_x p_0 + \bar{\omega}^2\mathbf{u}_0)$ , where  $\mathbf{P}$  and  $\mathbf{W}$  are linear operators. By volume averaging  $\mathbf{w}$  over the  $\mathbf{y}$  variable (pore scale) and denoting the result as  $\mathbf{U}$ , we get

$$\mathbf{U}=\langle\mathbf{W}(\mathbf{x},\mathbf{y})\rangle_y\cdot(\nabla_x p_0 + \bar{\omega}^2\mathbf{u}_0). \quad (3)$$

Since  $\nabla_x p_0$  may be regarded as the externally applied pressure gradient, Eq. (3) not only gives Darcy's law in the case of a rigid solid frame ( $\mathbf{u}_0=0$ ), but also tells us that to the first order, *solid displacement acts as an additional source excitation term and therefore does not enter the generic problem of permeability calculation*. By substituting the formal solutions of  $p_1$  and  $\mathbf{w}$  into Eq. (2), we finally obtain the general equations for the linear operators  $\mathbf{P}$  and  $\mathbf{W}$ :

$$-\nabla\mathbf{P} - i\bar{\omega}\nabla^2\mathbf{W} + \bar{\omega}^2\mathbf{W} = -\mathbf{I}, \quad (4a)$$

$$\nabla\cdot\mathbf{W}=0, \quad (4b)$$

with the condition that  $\mathbf{W}=0$  on pore-solid interfaces. Here we have dropped the subscript  $y$  on the gradient operators. From Eq. (3) it is seen that once  $\mathbf{W}$  is obtained from Eq. (4), the macroscopic permeability tensor  $\kappa(\omega)$  is given by

$$\kappa(\omega)=i\bar{\omega}\langle\mathbf{W}\rangle. \quad (5)$$

The  $\kappa$  tensor reduces to a scalar number in the case of

unidirectional, isotropic, or simple-cubic microstructure.

For a cylindrical tube with radius  $a$ , Eq. (4) can be solved analytically to get the known result<sup>9</sup>

$$\kappa(\bar{\omega})=ia^2/\bar{\omega}\{1-[2/(i\omega)^{1/2}]J_1((i\bar{\omega})^{1/2})/J_0((i\bar{\omega})^{1/2})\},$$

where  $\omega$  is in units of  $\eta/\rho_f a^2$ , and  $J_{0(1)}$  denotes the zeroth- (first-) order Bessel function. In restored units, the function  $\kappa$  has the following asymptotic frequency dependences<sup>4</sup> to the leading order:

$$\kappa=\begin{cases} AS+iBS^2(\rho_f/\eta)\omega, & \omega\rightarrow 0 \\ CS^{-1/2}(\eta/\rho_f)^{3/2}\omega^{-3/2}+iD(\eta/\rho_f)\omega^{-1}, & \omega\rightarrow\infty. \end{cases} \quad (6)$$

Here  $A$ ,  $B$ ,  $C$ , and  $D$  are dimensionless constants and  $S$  denotes the cross-sectional area. For  $\omega\rightarrow 0$ , the linear  $\omega$  dependence of the imaginary part comes from the ratio of the inertial to the viscous terms in Eq. (4a). For  $\omega\rightarrow\infty$ , the  $\omega^{-1}$  dependence is purely inertial [ $v\sim i\omega\omega\sim i\omega(\omega)^{-2}\sim i\omega^{-1}$ ] in origin, whereas the  $\omega^{-3/2}$  variation arises from a combination of the inertial effect plus the  $\omega^{-1/2}$  dependence of the viscous boundary layer thickness. The transition between the low- and the high-frequency regimes occur at  $\bar{\omega}\approx\frac{1}{4}$ . For straight tubes of noncircular cross sections, dimensional analysis tells us that only the constants  $A$ ,  $B$ ,  $C$ , and  $D$  are changed in Eq. (6). In fact, since the limiting frequency dependences arise from general considerations that are independent of the microstructure, they should be generic to the permeability function  $\kappa(\omega)$ . Therefore, for an arbitrary porous medium where  $S\neq\text{const}$ , we may write  $AS\rightarrow\kappa_0$  and  $BS^2\rightarrow C_1$ , i.e.,  $\kappa=\kappa_0+iC_1(\rho_f/\eta)\omega$  for low frequencies. At high frequencies, because of the fact that Eq. (4) can be transformed to a Laplace equation (for  $p$ ), the constant  $D^{-1}$  may be identified as the tortuosity factor  $\alpha$  that is electrically measurable,<sup>10</sup> and if one writes  $CS^{-1/2}$  as  $\sqrt{2}/\alpha\Lambda$ , then the length  $\Lambda$  has been identified as a weighted volume-to-surface ratio for the porous medium,<sup>2</sup> i.e.,

$$\kappa=\phi(\sqrt{2}/\alpha\Lambda)(\eta/\rho_f)^{3/2}\omega^{-3/2}+i\phi\alpha^{-1}(\eta/\rho_f)\omega^{-1},$$

for high frequencies.

To calculate  $\kappa(\omega)$  for porous media with arbitrary microstructures, Eq. (4) has to be solved numerically. Our calculations are divided into two parts. In the first part we consider periodic media with three different types of microstructures. The first one is a cylindrical pipe with sinusoidal modulation of its cross section, i.e.,  $S(z)=\pi a^2[1-(\delta/2)(1-\cos kz)]^2$ , where  $a$  is the maximum radius,  $\delta$  is a modulation parameter, and  $k$  gives the modulation periodicity. The second model is formed by the remains of spheres of radius  $a(1+\delta)$  after six caps of height  $a\delta$  have been cleaved off so they can be fitted on a simple cubic lattice with lattice constants  $2a$ . The third model is similar to the second one except the spheres are replaced by octahedrons of half-diagonal  $a(1+\delta)$  with six caps of heights  $a\delta$  cleaved off. It is

noted that  $\delta$  is a parameter that controls the porosity  $\phi$  and the microstructure in all three models. For the second part of the calculation, what has been learned about the characteristics of the various unit-cell microgeometries will be used to evaluate the permeability of a network of random permeable elements.

We have formulated a finite-element approach to the calculation of permeability in periodic models by discretizing the pore space into tetrahedron elements and using a fast band-matrix solver<sup>11</sup> for the simultaneous solution of  $\mathbf{w}$  and  $p$  at up to  $5 \times 10^4$  nodal points within an eighth of the unit cell. A complete run for a given structure consists of 10-15 different frequencies ranging from  $\bar{\omega}$  (in units of  $\eta/\rho_f a^2$ ) =  $10^{-2}$  to  $10^3$ . For the sake of accuracy, a separate Laplace-equation solver has been written to calculate the extreme high-frequency ( $\bar{\omega} \gg 1$ ) behavior. For the  $\delta=0$  case in model II, our value of  $\kappa_0$  is also checked to be within 2% of the one previously known calculation<sup>12</sup> of  $\kappa_0$ . Without exception, our results confirmed the generic asymptotic frequency dependence discussed earlier. That means that if we scale  $\kappa$  by  $\kappa_0$  and use  $\kappa_0$  as well as  $\alpha$  in our scaling of  $\omega$ , i.e.,  $\bar{\omega} = \omega/(\eta\phi/\rho_f\kappa_0\alpha)$ , then

$$\bar{\kappa}(\bar{\omega}) = \begin{cases} 1 + i(\alpha\kappa_0^2/C_1\phi)^{-1}\bar{\omega}, & \bar{\omega} \rightarrow 0, \\ \sqrt{2}(\Lambda^2\phi/\alpha\kappa_0)^{-1/2}\bar{\omega}^{-3/2} + i\bar{\omega}^{-1}, & \bar{\omega} \rightarrow \infty. \end{cases} \quad (7)$$

If the dimensionless combinations  $F_1 = \alpha\kappa_0^2/C_1\phi$  and  $F_2 = (\Lambda^2\phi/\alpha\kappa_0)^{1/2}$  remain constant under microstructural variations, then  $\bar{\kappa}(\bar{\omega})$  would exhibit universal asymptotic behavior. In Fig. 1 we plot all the numerical data for the three models and various  $\delta$  values in scaled variables. It is seen that in spite of drastic microstructural variations, the scaled data points collapse to a single curve not only at high and low frequencies, but also in the transition region as well. Indeed, while numerical evaluations of the parameters yield  $\kappa_0/a^2 \sim 10^{-4}-1$ ,  $C_1/a^4 \sim 10^{-7}-10^{-1}$ ,  $\Lambda/a \sim 0.1-1$ , and  $\alpha \sim 1-20$ , their dimensionless combination  $F_1$  gives a narrow range of 0.5-0.8 for its values and  $F_2 = 2.5-3$  for models I and II<sup>13</sup> and 5-7.3 for model III. Therefore, the four parameters  $\kappa_0$ ,  $C_1$ ,  $\Lambda$ , and  $\alpha$  can be recombined to yield  $\kappa_0$ ,  $\omega_c$ ,  $F_1$ , and  $F_2$ , with  $F_1$  and  $F_2$  approximately universal in their values.

We advance the following physical interpretation for this surprising result. The fluid flow rate  $Q$  at any given pore cross section can be written as  $Q = SU = S[(\kappa/\phi)/\eta]\Delta p/\Delta L$  by use of Darcy's law. If we write  $Q = R^{-1}\Delta p$ , then in analogy with electrical systems  $R = (\eta\phi/S\kappa)\Delta L$  may be regarded as flow resistance. If now  $S$  changes as a function of  $z$ , we can approximate each small segment  $\Delta L = \Delta z$  by a straight tube. By writing  $S = S(z)$  and  $\kappa = \kappa(z)$ , we get

$$R_{\text{eff}} = \eta\phi L \left[ \frac{1}{L} \int_0^L \frac{dz}{S(z)\kappa(z)} \right], \quad (8)$$

from which one gets  $\kappa_{\text{eff}} = \eta\phi L / \langle S \rangle R_{\text{eff}}$ , where the angu-

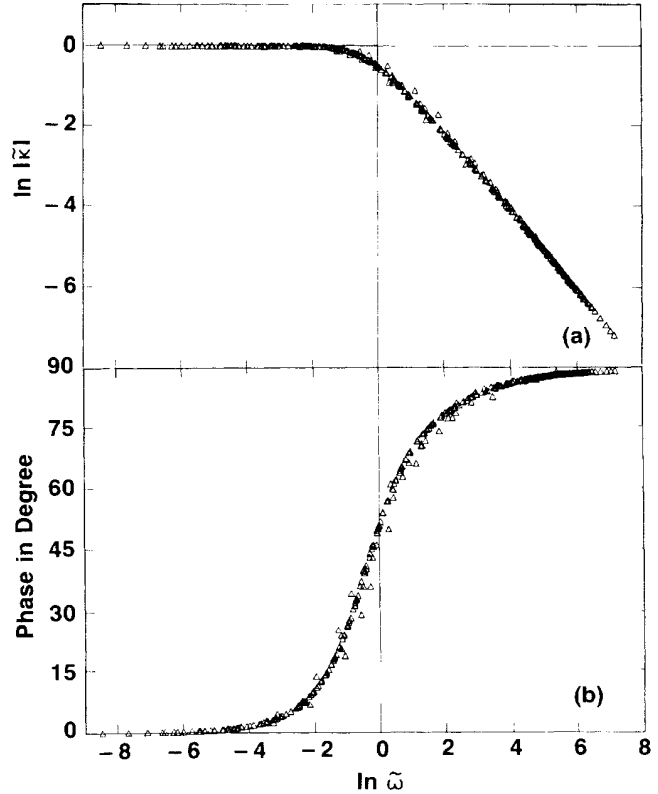


FIG. 1. (a) The magnitude and (b) the phase of the scaled dynamic permeability  $\bar{\kappa}(\bar{\omega})$ . A total of 22 sets of data are plotted. For model I,  $\delta=0.1, 0.2, 0.3, 0.4, 0.5, 0.55, 0.6, 0.65, 0.7, 0.75, 0.8, 0.85$ , and  $0.9$ . For model II,  $\delta=0, 0.1, 0.2, 0.25, 0.3, 0.35$ , and  $0.38$ . It should be noted that the throat area shrinks to zero at  $\delta = \sqrt{2} - 1 \approx 0.41$  for model II. For model III,  $\delta=0.6$  and  $0.8$ . The results that show the greatest deviations from scaling are those of model III for the reason discussed in the text. A line representing the solution for the straight tube would go through the middle of the scaled data points. The analytic model of  $\kappa(\omega)$  as given by Johnson, Koplik, and Dashen (Ref. 4) would also agree well with the collapsed data.

lar brackets denote averaging. If now one substitutes for  $\kappa(z)$  in Eq. (8) the asymptotic behavior of the tube solution, Eq. (6), then the asymptotic parameters  $\kappa_0$ ,  $C_1$ ,  $\Lambda$ , and  $\alpha$  for  $\kappa_{\text{eff}}$  have the following geometric interpretation:

$$\kappa_0 = \phi A / \langle S^{-2} \rangle \langle S \rangle, \quad (9a)$$

$$C_1 = B \langle S^{-1} \rangle / [\langle S^{-2} \rangle^2 \langle S \rangle], \quad (9b)$$

$$\Lambda = \sqrt{2} \langle S^{-1} \rangle / [C \langle S^{-3/2} \rangle], \quad (9c)$$

$$\alpha = \langle S^{-1} \rangle \langle S \rangle / D. \quad (9d)$$

Here it is assumed that the shape constants  $A$ ,  $B$ ,  $C$ , and  $D$  do not vary by orders of magnitude over the pore spaces (which is certainly valid for our periodic models) and therefore may be regarded as constants. In terms of Eq. (9),  $F_1 = A^2 / BD$  and

$$F_2 = (2D/C^2A)^{1/2} [\langle S^{-1} \rangle \langle S^{-2} \rangle / \langle S^{-3/2} \rangle^2]^{1/2}.$$

We recognize the fact that the average  $\langle S^{-n} \rangle$ , where  $n$  is a positive number, is always dominated by the throat area  $S_{th}$  when there is a large variation in the cross-sectional area. Therefore,  $F_1$  and  $F_2$  should stay relatively constant because  $F_1$  depends only on the shape constants and  $F_2$  cannot vary too much either since if  $S = \text{const}$ ,  $F_2 = (2D/C^2A)^{1/2}$ , and if  $S$  varies by a large factor, then  $\langle S^{-n} \rangle \approx S_{th}^{-n}$  and  $F_2$  again becomes dependent only on shape constants. In the same spirit,  $\Lambda$  is noted to be a volume-to-surface ratio for the throat region [Eq. (9c)] instead of the overall pore space. This line of argument demonstrates clearly that while the magnitudes of  $\kappa_0$ ,  $C_1$ , and  $\alpha$  are determined by more than just the throat area (since they also depend on  $\langle S \rangle$ ), there exist scaled variables  $\kappa, \omega$  so that when the geometry deviates most from a straight tube,  $\bar{\kappa}(\bar{\omega})$  is dominated by the throat and its overall behavior thereby returns to be straight-tube-like again. However, in order for the above description to be valid, the velocity vectors near the throat region must be nearly parallel so that one can use the approximation leading to Eq. (8). A situation that would violate this condition is where  $S(z)$  varies extremely fast as one moves away from the throat, e.g., two pores connected by a small hole in a thin sheet. In fact, we can detect small deviations from the scaling behavior for model III because  $dS/dz$  in the direction normal to the throat is large. For the other two models, on the other hand,  $dS/dz \approx 0$  in the throat region.

Can the scaling behavior seen in periodic structure be preserved in random systems? To answer this question we have carried out network calculations using permeable elements, each characterized by two parameters  $\kappa_0$  and  $\omega_c^{-1}$ . The parameter values are randomly sampled from a distribution function. By using exponential and log-normal distributions and solving essentially the Kirchhoff equations on  $5 \times 5 \times 5$  cubic lattices, we get results that clearly show scaling<sup>14</sup> and are indistinguishable from those in Fig. 1. We therefore conclude that as long as an individual element demonstrates scaling, the random network would exhibit the behavior as well. Previous calculations with tubes of random diameters have also supported this conclusion.<sup>4</sup>

The observed correlations between the product  $\kappa_0 \alpha$  and a measured throat size in sedimentary rocks<sup>3</sup> provide an indication that the condition for scaling may indeed be satisfied in naturally occurring materials. This can be seen by reference to Eqs. (9a) and (9d): Whereas both  $\kappa_0$  and  $\alpha$  depend on  $\langle S \rangle$ , their product is proportional to  $\langle S^{-1} \rangle / \langle S^{-2} \rangle \approx S_{th}$  as observed. Another evidence for the scaling behavior is provided by the

constancy of  $F_2$  for a variety of rocks as noted in Ref. 2.

In the succeeding experimental paper, it will be shown that the predictions of the theory are in excellent agreement with measured  $\kappa(\omega)$  for fused-glass-bead and crushed-glass samples. Together with the observed correlations in sedimentary rocks, they demonstrate that the condition for scaling is satisfied for a plurality of porous media and therefore only two independent pieces of microstructural information are generally obtainable from  $\kappa(\omega)$ . Furthermore, the knowledge about any combination of two parameters (such as  $\kappa_0$  and  $\alpha$ , or  $\alpha$  and  $\Lambda$ ) can yield predictions about the other two (by use of the  $F_1$  and  $F_2$  values) to within a factor of  $\sim 2$ . Experimental tests of these and other relations are described separately.<sup>5</sup>

---

(a)Permanent address: Department of Physics, Shanghai Teacher's University, Shanghai, People's Republic of China.

<sup>1</sup>A. H. Thompson, A. J. Katz, and C. E. Krohn, *Adv. Phys.* **36**, 625 (1987).

<sup>2</sup>D. L. Johnson, J. Koplik, and L. M. Schwartz, *Phys. Rev. Lett.* **57**, 2564 (1986).

<sup>3</sup>A. J. Katz and A. H. Thompson, *Phys. Rev. B* **34**, 8179 (1986).

<sup>4</sup>D. L. Johnson, J. Koplik, and R. Dashen, *J. Fluid Mech.* **176**, 379 (1987).

<sup>5</sup>E. Charlaix, A. P. Kushnick, and J. P. Stokes, following Letter [*Phys. Rev. Lett.* **61**, 1595 (1988)].

<sup>6</sup>R. Burridge and J. B. Keller, *J. Acoust. Soc. Am.* **70**, 1140 (1981). Our treatment of the  $\epsilon$  scaling differs from the reference above in that we treat  $\omega$  as an external parameter, and all the scaling units are taken from intrinsic constants of the medium.

<sup>7</sup>M. A. Biot, *J. Acoust. Soc. Am.* **34**, 1254 (1962).

<sup>8</sup>A complete consideration of all the first-order equations would yield Biot's equation as shown in Ref. 6.

<sup>9</sup>A. Bedford, R. D. Costley, and M. Stern, *J. Acoust. Soc. Am.* **76**, 1804 (1984).

<sup>10</sup>D. L. Johnson, T. J. Plona, C. Scala, F. Pasierb, and H. Kojima, *Phys. Rev. Lett.* **49**, 1840 (1982).

<sup>11</sup>Written by Bengt Fornberg. We wish to thank him for supplying us with this code.

<sup>12</sup>A. S. Sangani and A. Acrivos, *J. Multiphase Flow* **8**, 343 (1982).

<sup>13</sup>For straight tubes the value of  $F_2$  has been noted to be  $\sqrt{8} = 2.83$  in Ref. 4. It has also been noted in Ref. 2 that a variety of rocks and porous media give an almost universal value of  $F_2$  [ $= (8/M)^{1/2}$  in the notation of Ref. 4] that is  $\sqrt{8}$ .

<sup>14</sup>In the case of broad  $\omega_c$  and  $\kappa_0$  distributions, the physical reason for the scaling behavior may be constructed from the critical path argument as applied to permeability in Ref. 3.